This is an open access article published under an ACS AuthorChoice License, which permits copying and redistribution of the article or any adaptations for non-commercial purposes.

ACS Photonics

Article

pubs.acs.org/journal/apchd5

Single-Photon Quantum Contextuality on a Chip

Andrea Crespi,[†,‡] Marco Bentivegna,[¶] Ioannis Pitsios,[†,‡] Davide Rusca,[†] Davide Poderini,[¶] Gonzalo Carvacho,[¶] Vincenzo D'Ambrosio,[¶,§] Adán Cabello,[∥] Fabio Sciarrino,[¶] and Roberto Osellame*[,†,‡]

[†]Dipartimento di Fisica, Politecnico di Milano, p.za Leonardo da Vinci 32, 20133 Milano, Italy

[‡]Istituto di Fotonica e Nanotecnologie, Consiglio Nazionale delle Ricerche (IFN-CNR), p.za Leonardo da Vinci 32, 20133 Milano, Italy

[¶]Dipartimento di Fisica, Sapienza Università di Roma, p.le Aldo Moro 5, 00185 Roma, Italy

[§]ICFO - Institut de Ciencies Fotoniques, The Barcelona Institute of Science and Technology, 08860 Castelldefels (Barcelona), Spain

[∥]Departamento de Física Aplicada II, Universidad de Sevilla, 41012 Sevilla, Spain

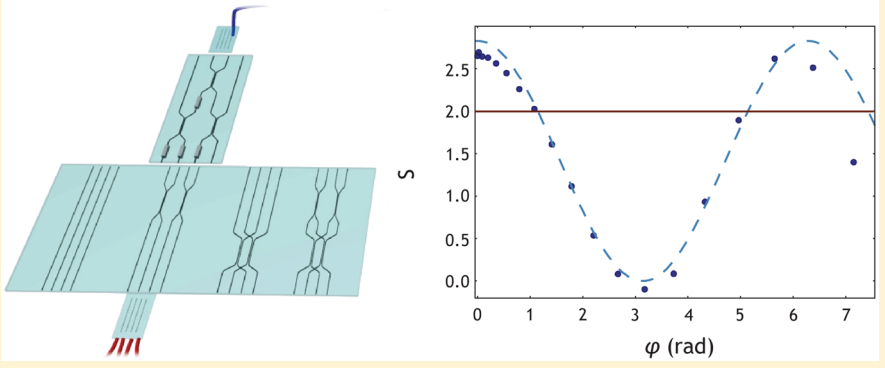

ABSTRACT: In classical physics, properties of objects exist independently of the context, i.e., whether and how measurements are performed. Quantum physics showed this assumption to be wrong, and that Nature is indeed "contextual". Contextuality has been observed in the simplest physical systems, such as single particles, and plays fundamental roles in quantum computation advantage. Here, we demonstrate for the first time quantum contextuality in an integrated photonic chip. The chip implements different combinations of measurements on a single photon delocalized on four distinct spatial modes, showing violations of a Clauser−Horne−Shimony−Holt (CHSH)-like noncontextuality inequality. This paves the way to compact and portable devices for contextuality-based quantum-powered protocols.

KEYWORDS: *integrated quantum photonics, femtosecond laser waveguide writing, quantum mechanics foundations, integrated optics, single photons*

Downloaded via UNIV DE SEVILLA on January 11, 2024 at 07:39:30 (UTC).
See https://pubs.acs.org/sharingguidelines for options on how to legitimately share published articles.

The assumption of noncontextuality, i.e., that measurements reveal properties that exist independently of whether and how measurements are carried out, lies at the heart of classical physics. The failure of this assumption in quantum theory[1,2] is dubbed "contextuality" and is a leading candidate for a notion of nonclassicality with broad scope. In fact, unlike Bell nonlocality,[3] contextuality applies not only to space-like separated composite systems but even to single particles. In addition, unlike macrorealism,[4] the set of noncontextual correlations has a precise mathematical definition.[5] The experimental observation of contextuality can be achieved by testing correlation inequalities,[6,7] which hold true whenever a noncontextual model exists and whose violation certifies that no noncontextual model is possible. A well-established approach to test quantum contextuality is based on sequential measurements operated on a single quantum system.[8−13] This kind of test generally assumes that measurements are sharp[14] (i.e., repeatable and minimally disturbing[15]) and that events (an event is a measurement and its outcome) have the same probability distributions in all preparation procedures,[16] even if it is possible to relax these idealizations by adopting an extended definition of noncontextuality.[17] This will be the approach followed in this work.

Many single-system quantum-contextuality-based schemes for cryptography[7,18,19] and randomness generation[20,21] have been proposed in recent years, and the mainstream interest in contextuality has skyrocketed after the proofs[22,23] that it constitutes the essential resource behind the power of certain quantum computers. Quantum optics is indeed a promising approach for the realization of actual quantum computing devices.[24] In particular, in the attempt to move toward scalable implementations of quantum computation and communication,

Received: July 20, 2017
Published: October 17, 2017

 © 2017 American Chemical Society

DOI: 10.1021/acsphotonics.7b00793
ACS Photonics 2017, 4, 2807−2812

a great deal of attention has been devoted to the development of integrated quantum photonics[25−31] in the past decade. In fact, the need for high-fidelity operations and increasing circuital complexity,[27,28] with a larger number of qubits, makes the use of integrated platforms an unavoidable choice in the long term. It is therefore of prime importance to investigate whether quantum contextuality can be produced in compact and integrable devices and specifically in quantum photonic chips.

Here we perform the first on-chip test of quantum contextuality. We work with a very essential physical system, in which a single degree of freedom of a single photon, i.e., its discretized spatial position on four modes, is used to encode two qubits. Reconfigurable photonic circuits, realized by femtosecond laser waveguide writing, are employed both to prepare delocalized photon states across the four modes and to implement different unitary operations, in order to achieve different projective measurements with the aid of single-photon detectors.

RESULTS AND DISCUSSION

To get an intuitive grasp on our experiment and on its implications, we shall first consider the mechanical toy model shown in Figure 1. This consists in a set of identical balls and a modified Galton board, composed of different sections, where the balls can be shuffled across four possible channels (A1, A2, B1, B2). The first section is a box with one input connected to four outputs; when we throw a ball in it, it comes out at one of the four outputs, according to a certain probability distribution, which is a function of the physical characteristics of the ball and of the box. We may look at this first box as a device that *prepares* the ball in a certain state. A second section of the apparatus is composed of two sliding parts that can be configured to perform different operations. Each of the sliding parts may just let the ball fall in the same channel as it enters (the Z operations) or introduce a 50% probability for a channel change (the X operations). M_{12} acts only on the digit, while N_{AB} acts only on the letter (M and N being either Z or X). Overall, there are four possible configurations for this second section. Balls are eventually collected at the output. We could consider the sliding sections, together with the collection stage, as an apparatus that allows performing different measurements on the prepared state, which yield as outcome two independent bits, a letter (A, B) and a digit (1, 2). Finally, we can conventionally assign a number (+1 or −1) to the outcomes of the two measurements, defined by the position of the two sliding parts as shown in Figure 1.

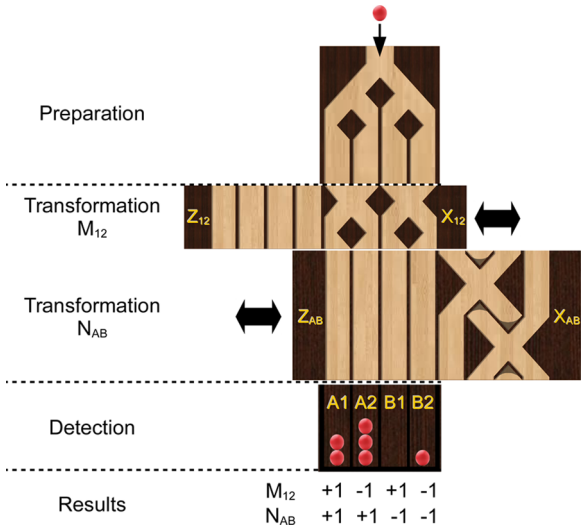

Figure 1. A mechanical example: identical balls enter a modified Galton board, composed of several sections. The first section distributes the balls in the four channels according to a certain probability distribution. That is, it prepares the balls in a certain state. The second section is reconfigurable and implements two transformations: M_{12} chosen between Z_{12} and X_{12}, and N_{AB} chosen between Z_{AB} and X_{AB}, depending on how the sliding parts are placed. Each of these transformations, together with the detection at the bottom, constitutes a measurement on the distribution prepared at the first stage, whose outcome is given by the final position of the ball as indicated in the figure. Note that the measurements corresponding to M_{12} and N_{AB} are always independent in the sense that the probabilities $P(N_{AB} = -1)$ and $P(N_{AB} = +1)$ are independent of M_{12}, and the probabilities $P(M_{12} = -1)$ and $P(M_{12} = +1)$ are independent of N_{AB}.

In this classical system, the position of the ball, although only probabilistically predictable, is always defined in every moment of its evolution. The following Clauser−Horne−Shimony−Holt (CHSH)-like noncontextuality inequality is therefore satisfied:[11]

$$S = \langle X_{12}X_{AB}\rangle + \langle X_{12}Z_{AB}\rangle + \langle Z_{12}X_{AB}\rangle - \langle Z_{12}Z_{AB}\rangle \leq 2 \quad (1)$$

where $\langle M_{12}N_{AB}\rangle$ is the average value of the product of the measurement outcomes of M_{12} and N_{AB} on a large number of events identically prepared. This inequality holds irrespectively of the specific features of the Z and X transformations, with the only condition that the operations implemented by the two moving parts are independent. This is intrinsically achieved since M_{12} and N_{AB} act on different bits.

The exact quantum analogue of the above classical mechanics experiment is performed by using photons instead of balls and integrated optical circuits instead of the wooden Galton board (Figure 2). Photons at 785 nm are provided by a heralded single-photon source, based on type-II spontaneous parametric down-conversion, which consists of a pulsed pump impinging on a beta barium borate (BBO) crystal. For each generated pair, one of the two photons acts as a trigger, while the second one is injected in a system of two cascaded integrated photonic chips, and the output is sent to single-photon detectors. Waveguides are inscribed in a borosilicate glass substrate using the femtosecond laser writing technology[29−31] (more details about the fabrication of the integrated devices are given in the Methods section). The first chip serves as the state preparation section. The second chip, together with the detectors at the output, allows us to perform several different measurements on the state. While in our mechanical example the four different possible measurements could be implemented by adjusting two moving parts (each with two allowed positions), here, for simplicity, we have fabricated four different photonic circuits, one next to the other, each implementing a different configuration. Relative translation of the second chip with respect to the first one allows selecting the desired measurement.

Quantum theory provides a clear description of our photonic experiment in terms of qubits and observables. In particular, the first chip prepares single photons in a superposition state of four spatial modes, which encodes two qubits. The first qubit identifies which half of the chip is occupied ($|0\rangle$ = left and $|1\rangle$ = right, as the letter in the classical example), and the second gives the parity of the occupied mode ($|0\rangle$ = odd and $|1\rangle$ =

DOI: 10.1021/acsphotonics.7b00793
ACS Photonics 2017, 4, 2807−2812

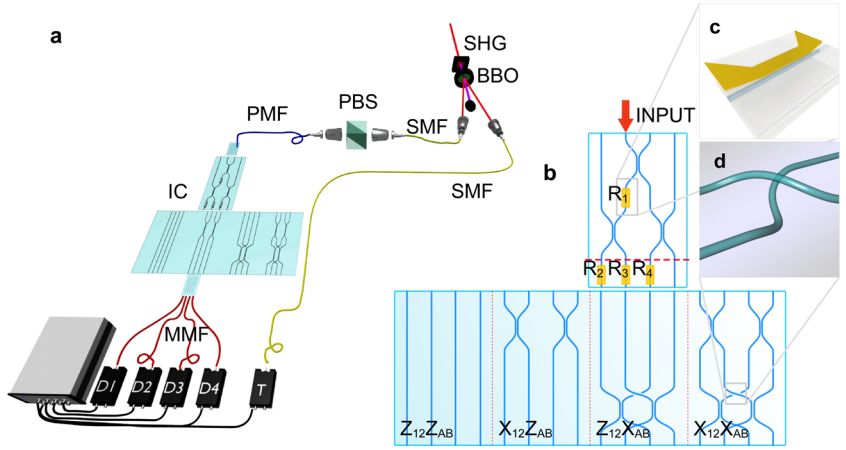

Figure 2. Experimental setup for the contextuality measurements. (a) The heralded single-photon source is based on second-harmonic generation by a pulsed laser beam on a first nonlinear crystal (SHG), followed by spontaneous parametric down-conversion on a BBO crystal. The generated photon pair is coupled to single mode fibers (SMF). The trigger photon is sent directly to a detector (T), while the signal photon is first passed through a polarizing beam splitter (PBS) and then coupled into a polarization maintaining fiber (PMF), which injects it into the integrated photonic circuits (IC). The four outputs are coupled to single-photon detectors (D1−D4) by an array of multimode fibers (MMF). Coincidence detection of the two photons is performed by an electronic board. (b) Detailed schematic of the two cascaded photonic chips: the first one serves as state preparation, while the second one implements different measurements on the single-photon state. Thermo-optic phase shifters (c) are deposited on the first chip to sweep through several different states (R1) and to calibrate the phase terms at the interface (R2, R3, and R4). The photonic circuits of the second chip exploit the three-dimensional capability of femtosecond laser waveguide writing (d), allowing the crossing of two waveguides without intersecting each other.

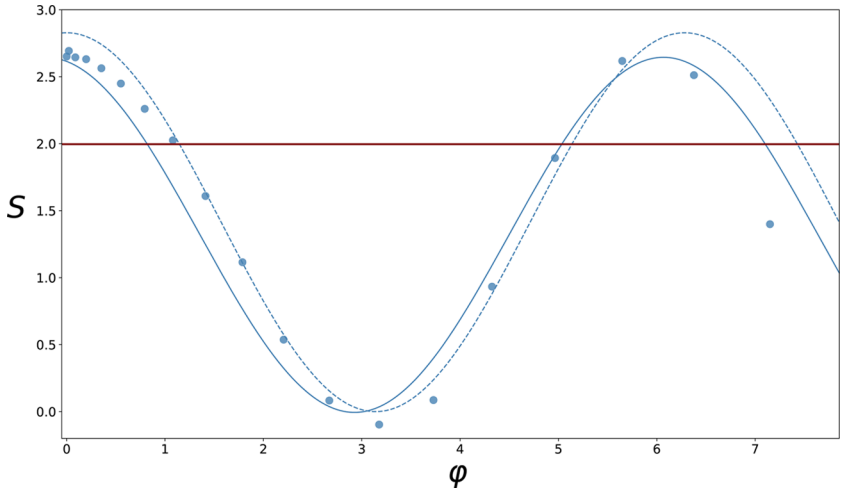

Figure 3. Observed values of the quantity S, left term of inequality 1, as a function of the input state phase φ (in radians). Blue points are experimental values. The dashed line corresponds to theoretical prediction of quantum mechanics in the case of ideal devices for state preparation and measurements, while the continuous line shows the theoretical prediction taking into account the effective transmissivities of the beam splitters in the implemented devices, as inferred from the characterization performed with classical light. The noncontexuality bound $S = 2$ is marked with the horizontal red line.

even, as the digit in the classical example). The four states ($|00\rangle$, $|01\rangle$, $|10\rangle$, and $|11\rangle$) correspond to the states with the photon in a well-defined spatial mode. The preparation chip includes three cascaded directional couplers properly designed to produce photons in the state:

$$|\psi\rangle = \frac{|00\rangle e^{i\varphi} + (1 + \sqrt{2})(|01\rangle e^{i\varphi} + |10\rangle) - |11\rangle}{2\sqrt{2 + \sqrt{2}}} \quad (2)$$

where the term φ can be varied by a thermo-optic phase shifter, marked as R1 in Figure 2b. The above photon state is defined in the circuit at the red dashed line reported in the same figure. Three further thermo-optic shifters (R2, R3, and R4) enable a fine-tuning of the optical path-lengths in the different output branches to compensate for slight geometrical misalignments when the two chips are coupled together.

The second chip, together with the fiber-coupled single-photon detectors, allows us to perform the different measurements required to evaluate the CHSH-like inequality 1. The Z and X operations are implemented respectively with straight waveguides, which let the photons proceed straight on the same modes, and balanced directional couplers, which enable mode-hopping of the photon between two modes with 50% probability. In quantum theory, such transformations are equivalent to basis rotation on the eigenbasis of the Pauli operators σ_z and σ_x. The Z operation leaves a qubit unchanged, so that measuring an output photon in the left or in the right mode corresponds to measuring the states $|0\rangle$ and $|1\rangle$. The X

DOI: 10.1021/acsphotonics.7b00793
ACS Photonics 2017, 4, 2807−2812

operation, which consists in the Hadamard gate, switches from the σ_Z basis to the σ_X one and vice versa, allowing one to measure in the $\{|-\rangle, |+\rangle\}$ basis by detecting photons in the left or right mode. By combining σ_X and σ_Z operators we can build the four observables $X_{12}X_{AB} = \sigma_X \otimes \sigma_X$, $X_{12}Z_{AB} = \sigma_X \otimes \sigma_Z$, $Z_{12}X_{AB} = \sigma_Z \otimes \sigma_X$, and $Z_{12}Z_{AB} = \sigma_Z \otimes \sigma_Z$, where $\sigma_j \otimes \sigma_i$ means σ_i and σ_j acting on the first and the second qubit, respectively. The generic term $\langle M_{12}N_{AB}\rangle$ in the inequality 1 (M and N being either X or Z) is given by $P_1^{MN} - P_2^{MN} - P_3^{MN} + P_4^{MN}$, where P_i^{MN} is the probability of finding a photon in mode i after operating the transformation M on the first qubit and N on the second. It should be noted that the quantum operations performed by the second chip can be fully characterized using coherent light.

The actual experiment is performed by collecting coincidence counts between the trigger detector and one of the output detectors for several values of dissipated power in the resistance R1 (i.e., for different phases φ of the input state (eq 2)) and for each of the four possible measurement configurations. The experimental results are shown in Figure 3 (full circles): each point corresponds to a different contextuality experiment performed with a different input state. The dashed line in the graph represents the expectation value of S according to quantum mechanics, in an experiment performed with ideal devices. Consistently with the predictions of quantum theory, a violation of the noncontextuality classical bound $S \leq 2$ is evident for the points around $\varphi = 0$ or $\varphi = 2\pi$. It can be noted that the experimental points do not reach the maximum value of S predicted by the theory. This feature can be explained by the fabrication imperfections of our integrated photonic components. A more realistic quantum mechanical model that relies on measured beam splitter transmissivities better fits the experimental points (continuous line in Figure 3). Residual disagreement between the experimental points and the adapted model can be attributed to other sources of imperfections, such as suboptimal phase tuning and alignment between the two chips, which are difficult to estimate precisely.

Experimental imperfections in implementing the measurements, however, not only modify the expected quantum mechanical behavior but also extend the range of S values that can be explained classically, thus raising the bound for quantum contextuality. In particular, in our experiment the use of different circuits to measure the same physical quantity in the different terms of eq 1 may introduce nonideality in the measurements (see Methods). A recent work by Kujala et al.[17] proposes a modified inequality:

$$S \leq 2 + \varepsilon \tag{3}$$

where $\varepsilon \geq 0$ includes the effect of such nonideality in a worst-case scenario. The approach of ref 17 is powerful because ε can be evaluated directly from the same experimental data set used to calculate S (see the Methods section for details). Thus, for each experimental point it is possible to calculate a specific bound, which, importantly, does not rely on supplementary characterizations of the experimental apparatus or other assumptions that may introduce further errors.

Figure 4 compares the measured values of S for the input states with $0 \leq \varphi < 0.6$ (i.e., the ones close to the point of maximal predicted violation) with the modified classical bounds, indicated by the height of the blue columns. One can observe how this correction can be quite relevant and different for each point. Each point corresponds indeed to a different and completely independent quantum contextuality experiment, where small imperfections in the alignment

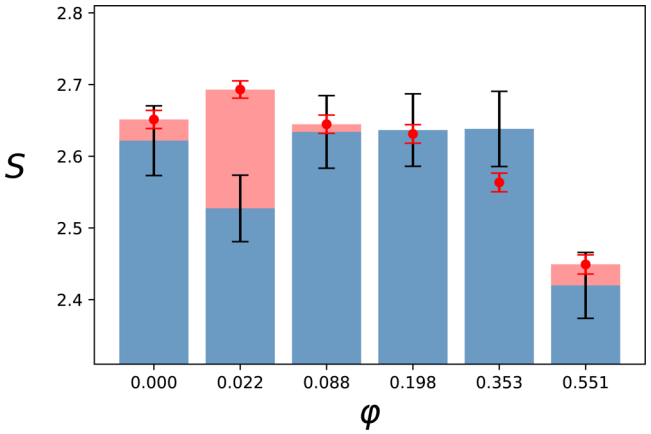

Figure 4. Experimentally measured values for S (red circles) for the input states close to $\varphi = 0$, compared to the corrected noncontextuality bound (blue columns) as given by eq 3. The red columns, where present, highlight the amount of contextuality that cannot be explained classically. 1σ error bars are also shown, derived assuming Poissionian statistics in the collected photon coincidences.

between the two chips and in tuning the phases at the interface are found to influence critically the corrected bound. For certain points (e.g., $\varphi = 0.198$ or $\varphi = 0.353$), even if S is significantly larger than 2, and the results are consistent with the quantum theory (see Figure 3), we cannot overcome this corrected bound and thus rule out completely a classical explanation. However, for the experiment performed with $\varphi = 0.022$, the measured value $S = 2.69 \pm 0.012$ violates plainly the corrected bound with a 99.5% confidence (calculated as in ref 17). The probability that all six experimental points shown in Figure 4 are below the bounds, i.e., the probability that no violation of classicality has been observed in any of those experiments, is lower than 5×10^{-6} (excluding the point at $\varphi = 0.022$, the probability that no violation has been observed in the other five points shown in Figure 4 is still below 0.02). Therefore, even taking into account the experimental imperfections, the results cannot be explained by a classical noncontextual model.

It is interesting to compare the behavior of the mechanical setup of Figure 1 to the results of our experiment in integrated quantum photonics. In fact, in the first case the physical state of the ball is described not only by its position but also by many other quantities (its shape, its speed, its orientation, etc.), which are a sort of hidden variables. Randomness there is due to ignorance of these hidden variables. Within a classical description, a perfect knowledge of all the parameters would instead allow predicting exactly the output channel for each ball we throw in, whatever measurement is performed. On the contrary, in our photonic experiment, according to quantum theory, the only available degree of freedom for the photons in each point of their propagation inside the chips is their position, namely, which optical mode they populate. However, even if we knew precisely this information at the initial condition, i.e., in which mode the photon is injected, quantum theory would not predict exactly at which output mode the photon will exit. In fact, the occupation of any mode by the photon will remain undetermined up to the point at which it is measured. This substantial difference from the classical description is the main reason for the experimental violation of the inequality 1 by a quantum system, thus forbidding the

DOI: 10.1021/acsphotonics.7b00793
ACS Photonics 2017, 4, 2807−2812

existence of noncontextual hidden variables that would determine a specific trajectory for each photon in the device.

In conclusion, we have shown the first contextuality test on an integrated photonic chip, demonstrating the reliability and versatility of current photonic integration techniques for testing quantum properties and for producing compact and portable devices capable of exploiting and certifying the enhanced capabilities of quantum technologies. In perspective, this technology could be used to implement sources of correlations with computational power[32] integrable within conventional hardware.

We highlight that the intrinsic stability of integrated waveguide circuits has allowed us to design and perform an experiment involving only the spatial degree of freedom of a single photon and in particular based only on interference between different paths. Our experimental setup thus makes it easy to visualize that contextuality is a fundamental property of quantum systems and a direct consequence of wave function interference.

METHODS

Derivation of the Inequality. The CHSH-like inequality 1 holds true on three fundamental assumptions:

- *Realism*: The outcomes of a measurement are determined *before* the actual measurement.
- *Noncontextuality*: The outcome of a measurement does not depend on which others *compatible* measurment(s) are simultaneously performed.
- *Compatibility*: The four couples of observables

$$(X_{12}, X_{AB})(X_{12}, Z_{AB})$$
$$(Z_{12}, X_{AB})(Z_{12}, Z_{AB})$$

are compatible.

The notion of compatibility outside of the framework of quantum mechanics needs clarification. Here we call two measurements *compatible* when they can be measured simultaneously without any disturbance.

If the above assumptions are satisfied, knowing that the measurement outcomes of the observables can only take the values ± 1, it is easy to see that the left-hand side of eq 1 can never exceed 2. Therefore, if a violation of the inequality is experimentally observed, it follows that one of the above assumptions is not satisfied. In particular our experiment aims at disproving the combination of the first two, called *noncontextual realism*, by ensuring that the third holds true. This means that the measurement of M_{12} (or N_{AB}) made jointly with Z_{AB} (or Z_{12}) should yield the same result as the one made with X_{AB} (or X_{12}), for every input state.

Nonideality. The right-hand side of the CHSH-like inequality 1 is derived under the assumption that each measurement has identical probability distributions in the two contexts. However, this does not hold in any real experiment, either because of a contextually biased measurement design, as is the case of our experiment, or because experimental imperfections give rise to apparent signaling.

As explained in ref 17, it is possible to derive a different bound for the inequality, whose violation certifies contextuality even when these nonidealities are taken into account. Namely, the new bound for eq 1 becomes

$$S \leq 2 + \varepsilon$$
$$\varepsilon = \sum_{M} |\langle M^X \rangle - \langle M^Z \rangle|$$

where we have introduced the notation M^N to distinguish the measurement M performed simultaneously with N, and the sum is extended to the four measurements X_{12}, X_{AB}, Z_{12}, and Z_{AB}. Note that the values of different $\langle M^N \rangle$ can be retrieved from the same set of experimental data used to evaluate eq 1.

Waveguide Fabrication. Waveguides were fabricated by direct femtosecond laser writing using a Yb:KYW cavity-dumped mode-locked oscillator (λ = 1030 nm). Ultrafast pulses (300 fs pulse duration, 1 MHz repetition rate) were focused using a 0.6 NA, 50× microscope objective into the transparent volume of an alumino-borosilicate glass (Corning, EAGLE 2000), producing a local and permanent refractive index increase. Translation of the sample with a constant tangential velocity of 40 mm s^{-1} (Aerotech FiberGLIDE 3D air-bearing stages) allows drawing the desired waveguiding paths. In the state preparation chip, waveguides were inscribed at 25 μm depth, with 220 nJ pulse energy. In the measurement chip, waveguides were inscribed at 70 μm depth and 230 nJ pulse energy. The size of the two chips is respectively 49 mm × 24 mm and 65 mm × 27 mm. The thermo-optic phase shifters are fabricated by depositing a thin gold layer on the top surface of the chip and by patterning the resistors by laser ablation, with the same femtosecond laser source used for the waveguide fabrication (according to the method described in ref 31). This kind of device is able to control phase shifts without drifts and within 0.01 rad standard deviation, on a time-scale of several hours.[31]

AUTHOR INFORMATION

Corresponding Author

*E-mail: roberto.osellame@polimi.it.

ORCID

Roberto Osellame: 0000-0002-4457-9902

Notes

The authors declare no competing financial interest.

ACKNOWLEDGMENTS

This work was financially supported by the European Research Council (ERC) Starting Grant 3D-QUEST (3D-Quantum Integrated Optical Simulation; grant agreement no. 307783, http://www.3dquest.eu), by the H2020-FETPROACT-2014 Grant QUCHIP (Quantum Simulation on a Photonic Chip; grant agreement no. 641039, http://www.quchip.eu), and by the Marie Curie Initial Training Network PICQUE (Photonic Integrated Compound Quantum Encoding, grant agreement no. 608062, FP7-PEOPLE-2013-ITN, http://www.picque.eu). A.Ca. acknowledges support from Project No. FIS2014-60843-P, "Advanced Quantum Information" (MINECO, Spain), with FEDER funds and the project "Photonic Quantum Information" (Knut and Alice Wallenberg Foundation, Sweden). G.C. thanks Becas Chile and Conicyt for a doctoral fellowship.

REFERENCES

(1) Bell, J. S. On the problem of hidden variables in quantum mechanics. *Rev. Mod. Phys.* **1966**, *38*, 447−452.

(2) Kochen, S.; Specker, E. P. The problem of hidden variables in quantum mechanics. *J. Math. Mech.* **1967**, *17*, 59−87.

DOI: 10.1021/acsphotonics.7b00793
ACS Photonics 2017, 4, 2807−2812

(3) Bell, J. S. On the Einstein Podolsky Rosen paradox. *Physics* **1964**, *1*, 195−200.
(4) Clemente, L.; Kofler, J. No Fine Theorem for Macrorealism: Limitations of the Leggett-Garg Inequality. *Phys. Rev. Lett.* **2016**, *116*, 150401.
(5) Araújo, M.; Quintino, M. T.; Budroni, C.; Terra Cunha, T.; Cabello, A. All noncontextuality inequalities for the *n*-cycle scenario. *Phys. Rev. A: At., Mol., Opt. Phys.* **2013**, *88*, 022118.
(6) Aspect, A.; Dalibard, J.; Roger, G. Experimental Test of Bell's Inequalities Using Time-Varying Analyzers. *Phys. Rev. Lett.* **1982**, *49*, 1804−1807.
(7) Spekkens, R. W.; Buzacott, D. H.; Keehn, A. J.; Toner, B.; Pryde, G. J. Preparation Contextuality Powers Parity-Oblivious Multiplexing. *Phys. Rev. Lett.* **2009**, *102*, 010401.
(8) Cabello, A. Experimentally Testable State-Independent Quantum Contextuality. *Phys. Rev. Lett.* **2008**, *101*, 210401.
(9) Lapkiewicz, R.; et al. Experimental non-classicality of an indivisible quantum system. *Nature* **2011**, *474*, 490−493.
(10) D'Ambrosio, V.; et al. Experimental implementation of a Kochen-Specker set of quantum tests. *Phys. Rev. X* **2013**, *3*, 011012.
(11) Hasegawa, Y.; Loidl, R.; Badurek, G.; Baron, M.; Rauch, H. Violation of a Bell-like inequality in single-neutron interferometry. *Nature* **2003**, *425*, 45−48.
(12) Kirchmair, G.; et al. State-independent experimental test of quantum contextuality. *Nature* **2009**, *460*, 494−497.
(13) Moussa, O.; Ryan, C. A.; Cory, D. G.; Laflamme, R. Testing Contextuality on Quantum Ensembles with One Clean Qubit. *Phys. Rev. Lett.* **2010**, *104*, 160501.
(14) Spekkens, R. W. The status of determinism in proofs of the impossibility of a noncontextual model of quantum theory. *Found. Phys.* **2014**, *44*, 1125−1155.
(15) Chiribella, G.; Yuan, X. Measurement sharpness cuts nonlocality and contextuality in every physical theory. arXiv:1404.3348, 2014.
(16) Spekkens, R. W. Contextuality for preparations, transformations, and unsharp measurements. *Phys. Rev. A: At., Mol., Opt. Phys.* **2005**, *71*, 052108.
(17) Kujala, J. V.; Dzhafarov, E. N.; Larsson, J. Å. Necessary and Sufficient Conditions for an Extended Noncontextuality in a Broad class of Quantum Mechanical Systems. *Phys. Rev. Lett.* **2015**, *115*, 150401.
(18) Ekert, A. K. Quantum Cryptography Based on Bell's Theorem. *Phys. Rev. Lett.* **1991**, *67*, 661−663.
(19) Cabello, A.; D'Ambrosio, V.; Nagali, E.; Sciarrino, F. Hybrid ququart-encoded quantum cryptography protected by Kochen-Specker contextuality. *Phys. Rev. A: At., Mol., Opt. Phys.* **2011**, *84*, 030302R.
(20) Pironio, S.; et al. Random numbers certified by Bell's theorem. *Nature* **2010**, *464*, 1021−1024.
(21) Um, M.; et al. Experimental certification of random numbers via quantum contextuality. *Sci. Rep.* **2013**, *3*, 1627.
(22) Howard, M.; Wallman, J.; Veitch, V.; Emerson, J. Contextuality supplies the 'magic' for quantum computation. *Nature* **2014**, *510*, 351−355.
(23) Delfosse, N.; Guerin, P. A.; Bian, J.; Raussendorf, R. Wigner Function Negativity and Contextuality in Quantum Computation on Rebits. *Phys. Rev. X* **2015**, *5*, 021003.
(24) Ladd, T. D.; Jelezko, F.; Laflamme, R.; Nakamura, Y.; Monroe, C.; O'Brien, J. L. Quantum computers. *Nature* **2010**, *464*, 45−53.
(25) Politi, A.; Cryan, M.; Rarity, J.; Yu, S.; O'Brien, J. Silica-on-silicon waveguide quantum circuits. *Science* **2008**, *320*, 646.
(26) Tanzilli, S.; Martin, A.; Kaiser, F.; De Micheli, M.; Alibart, O.; Ostrowsky, D. On the genesis and evolution of Integrated Quantum Optics. *Laser Photon. Rev.* **2012**, *6*, 115−143.
(27) Carolan, J.; et al. Universal linear optics. *Science* **2015**, *349*, 711−716.
(28) Bentivegna, M.; et al. Experimental scattershot boson sampling. *Sci. Adv.* **2015**, *1*, e1400255.
(29) Marshall, G. D.; et al. Laser written waveguide photonic quantum circuits. *Opt. Express* **2009**, *17*, 12546−12554.
(30) Sansoni, L.; et al. Polarization entangled state measurement on a chip. *Phys. Rev. Lett.* **2010**, *105*, 200503.
(31) Flamini, F.; et al. Thermally reconfigurable quantum photonic circuits at telecom wavelength by femtosecond laser micromachining. *Light: Sci. Appl.* **2015**, *4*, e354.
(32) Anders, J.; Browne, D. E. Computational Power of Correlations. *Phys. Rev. Lett.* **2009**, *102*, 050502.

DOI: 10.1021/acsphotonics.7b00793
ACS Photonics 2017, 4, 2807−2812